

Corrugated Band-Notched Antipodal Vivaldi Antenna using Mushroom Type EBG Structure for Wideband Applications

Open
Access

Saidu Adamu Abubakar^{1,*}, Thelaha Hj Masri¹, Wan Azlan Wan Zainal Abidin¹, Kismet Hong Ping¹, Hieng Tiong Su²

¹ Department of Electronics Engineering, Faculty of Engineering Universiti Malaysia Sarawak, 94300 K/Samarahan, Malaysia

² Faculty of Engineering, Computing and Science, Swinburne University of Technology, 93350 Kuching, Malaysia

ARTICLE INFO

ABSTRACT

Article history:

Received 23 September 2018

Received in revised form 18 November 2018

Accepted 20 December 2018

Available online 23 December 2018

An Ultra wideband (UWB) Corrugated Antipodal Vivaldi Antenna operating at 2.29 GHz to more than 12 GHz having dual band-notch characteristics is designed for wideband applications. The proposed double-layered AVA is designed using a low cost FR-4 dielectric substrate with combined thickness of 2.1mm. Two edge-located vias mushroom type electromagnetic band gap (EBG) structures were designed and incorporated in to a corrugated conventional antipodal Vivaldi antenna (CAVA) in between the two substrate layers and below the feeding line, to realize the proposed antenna. Using the band gap property of the EBG structure, two notch bands were created within the ultra wideband frequency range of the antenna for IEEE 802.16 WiMAX application at 3.21 – 3.80 GHz and IEEE 802.11a WLAN application at 5.12 – 5.80 GHz. Simulation and measured results agreed well, with nearly stable end-fire radiation patterns in the entire frequency range except in the two notch bands with a peak realize gain of 8.04 dBi at 6.5 GHz. Surface current distribution and far-field radiation patterns are also studied to further characterize the performance of the proposed antenna.

Keywords:

Antipodal Vivaldi antenna, band-notch, edge-located vias, electromagnetic band gap structures, slot edge corrugation, ultra wideband

Copyright © 2018 PENERBIT AKADEMIA BARU - All rights reserved

1. Introduction

Rapid increase has being witnessed in the use of the ultra wideband frequency spectrum and quite a number of UWB antenna designs has been proposed in both the academia and the industry following the commercial licensing of the UWB frequency spectrum by the federal communication commissions (FCC) in February 2002 [1]. After the release of the UWB frequency spectrum of 3.1 – 10.6 GHz for commercial use, interest grew in the use of this spectrum for both military and industrial wireless communication applications [1]. UWB antennas such as log-periodic, TEM horn, fractal, spiral, bow-tie, conical and Vivaldi antennas [2,3] have being investigated and proposed.

* Corresponding author.

E-mail address: aqi@gmail.com (Saidu Adamu Abubakar)

Desirable electrical features such as planar and simple structure, light weight and low profile, symmetric beam in both radiating planes, and conformity with mounting host surfaces [4-7] among others have combined to make the Vivaldi antenna more competitive in UWB applications compared other UWB antennas such as the Log periodic and the Horn antennas, which are very bulky and non-planar. The Vivaldi antenna was first proposed by Gibson [8] as a travelling wave, coplanar tapered slot antenna, before being successively improved by Gazit [9] and then Langley [10] in order to overcome the limitations of the initial design.

The unique characteristics of the Vivaldi antenna has enabled its deployment in applications such as detection of cancerous cells and tumors [11,12], microwave imaging of structures and construction materials [13-16], for high range radar systems [17], see through wall applications [18] and many other applications. Within the specified 3.1 – 10.6 GHz UWB frequency spectrum also existed other narrow band wireless technologies including IEEE 802.16 WiMAX standard at 3.5 GHz (3.3 – 3.8 GHz) and the IEEE 802.11a WLAN standard at 5.5 GHz (5.15 – 5.825 GHz), which might cause possible electromagnetic interference to the UWB applications. The need thus arise for extra circuitry in the UWB antenna covering the whole range of the UWB frequency band to filter out the band of frequencies that might cause the potential interference to the UWB system operation.

However, due to the non-uniformity of the Vivaldi antenna radiators which are of elliptical or exponential taper shape, precious little investigation of band-notch Vivaldi antennas have being reported [19-23] for single or multiple frequencies band-notched. An Ω -shaped slot and a U-shaped slot where etched on the radiating arms of the AVA in [19] and [20] respectively to realize a frequency band-notch at 5.5 GHz WLAN. Following similar approach, a capacitive loaded loop (CLL) resonator [21] was inserted to a UWB Vivaldi antenna for band-notch operation at the same WLAN frequency. In addition to only one band-notch being created, using these perturbation techniques to create the band-notch degrades the radiation pattern and efficiency of the UWB antenna. A band-notch of 5 - 6 GHz was equally achieved in [22] with an elliptically-tapered miniaturized slot antenna. Though this antenna has small size, it however, only provides a single notch at IEEE 802.11a WLAN band with an undesired H-plane radiation pattern. A band-notch for WiMAX application from 3.3 – 3.6 GHz was also obtained using a resonant parallel strip (RPS) loaded AVA [23]. However, the location of the RPS negatively impacts the design complexity of the antenna in addition to only one notch frequency band being realized. Using two pairs of EBG cells along the AVA feed line, [24] achieved two band-notches for WiMAX and ISM bands at 3.6 – 3.9 GHz and 5.6 – 5.8 GHz respectively which however have a wide bandwidth between the stop band and the usable frequency.

In this paper a double-layered dual band-notch corrugated AVA is designed using the edge-located vias mushroom type EBG structure. By introducing the EBG structure between the two layers of the antenna a dual band-notch of 3.21 – 3.80 GHz (for IEEE 802.16 WiMAX) and 5.12 – 5.80 GHz (IEEE 802.11a WLAN) can be easily achieved. Flexibility with respect to controlling the number and location of the stop band frequencies for antennas with non-uniform radiators such the AVA can be realized using this design method.

2. Methodology

2.1 Antenna Geometric Design

Figure 1 shows the development of the proposed antenna. A conventional AVA Figure 1(a) is designed on a double-layered inexpensive fire retardant -4 (FR4) dielectric substrate having relative permittivity (ϵ_r) of 4.4, dielectric loss tangent $\delta = 0.019$ and a combined thickness (h_1+h_2) of 2.1mm.

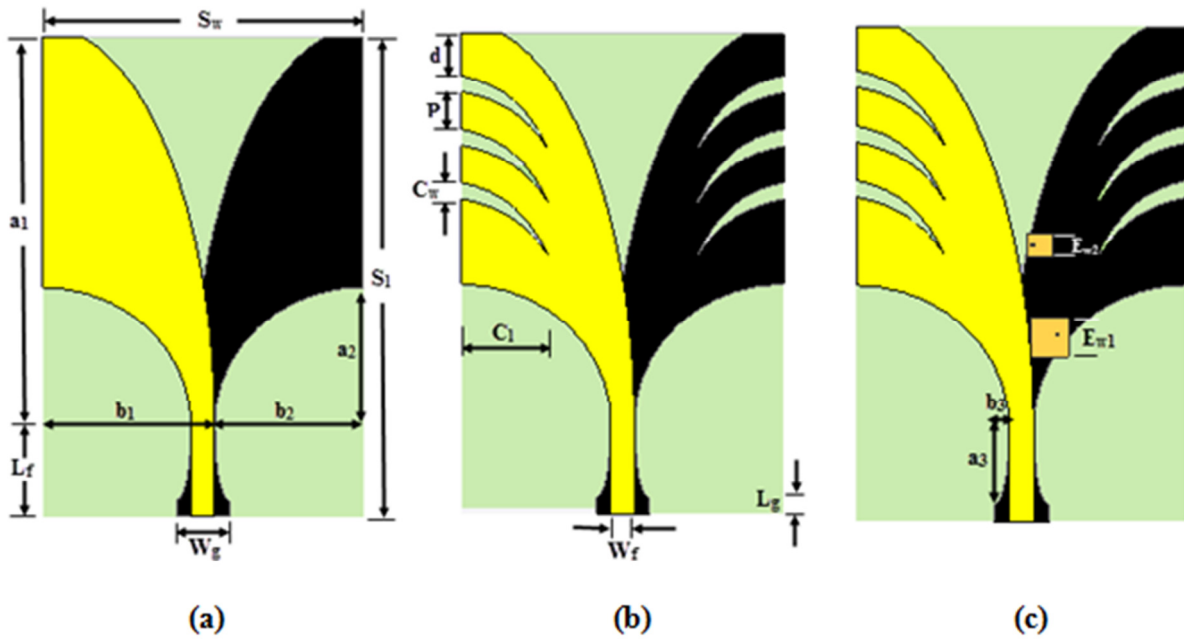


Fig. 1. (a) Conventional AVA (b) Corrugated AVA (c) Proposed AVA

As a consequence of its simple structure and smooth transition between the radiating flare and the feed line, and because it provides a wide impedance bandwidth, the taper of the radiating arm follows the elliptical shape in which the radii of the outer and inner quarter ellipses are defined by

$$a_1 = (S_l - L_f) + k \tag{1}$$

$$a_2 = 0.347a_1 \tag{2}$$

$$a_3 = (L_f - L_g) \tag{3}$$

$$b_1 = \frac{S_w + W_f}{2} \tag{4}$$

$$b_2 = \frac{S_w - W_f}{2} \tag{5}$$

$$b_3 = \frac{W_g - W_f}{2} \tag{6}$$

where; S_l is the substrate length, S_w the substrate width, W_f the feed line width, W_g the ground plane width, L_f the feed line length and L_g the ground plane length. For the ellipses, a_1 , a_2 and a_3 represents the major radii of outer, inner and ground plane ellipses, while b_1 , b_2 and b_3 are the secondary radii of outer, inner and ground plane ellipses respectively. k represents a constant that determines the aperture width.

The upper frequency limit has a theoretically infinite value whereas the width of the antenna at the open aperture determines the lower end frequency limit which was obtained from

$$f_{\min} = \frac{c}{2W\sqrt{\epsilon_{\text{eff}}}} \tag{7}$$

where:

$$\epsilon_{eff} = \frac{\epsilon_r + 1}{2} + \frac{\epsilon_r - 1}{2} \left(1 + \frac{12h}{W} \right)^{-\frac{1}{2}} \quad (8)$$

where ϵ_{eff} is the effective permittivity and W represents the aperture width.

To miniaturize the antenna and improve the impedance bandwidth, corrugation was loaded on both sides of the radiating flare by cutting exponential slots of equal dimension from the copper of the radiating arm as shown in Figure 1(b). Edge-located vias mushroom type EBG cells were then designed and incorporated in between the two substrate layers and under the feed line to realize the proposed antenna as shown in Figure 1(c) and achieve the band notch at the specified frequency bands. The optimize parameters of the antenna and the EBG structure are given in Table 1.

Table 1
Optimized parameters of the proposed antennas and EBG structures

Vivaldi Antenna				EBG ₁		EBG ₂	
Parameter	Value (mm)	Parameter	Value (mm)	Parameter	Value (mm)	Parameter	Value (mm)
S_l	90	a_1	75	EW_1	7	EW_2	4.5
S_w	60	a_2	26	Vr_1	0.3	Vr_2	0.3
W_f	4.4	a_3	14	g_1	1.5	g_1	1
W_g	10	b_1	32.2	g_2	8	g_2	3
L_g	3	b_2	27.8	x_{dist}	5	x_{dist}	1
L_f	17	b_3	2.8	y_{dist}	3	y_{dist}	2.25

2.2 Notch Band Implementation

As artificial periodic structures, the electromagnetic band gap (EBG), upon interaction with electromagnetic waves produces thrilling phenomenon in the form of pass band, stop band and a band gap where they act as artificial magnetic conductor. Thus the band gap property is used here to create the frequency band notch of the presented antenna. Therefore, for obtaining the band notches at 3.5 GHz WiMAX and 5.5 GHz WLAN bands two edge-located vias mushroom type EBG structure are designed and incorporated to the corrugated AVA as shown in Figure 1(c). The notch frequencies are given by

$$f_i = \frac{1}{2\pi\sqrt{L_i C_i}} \quad (9)$$

where; $i = 1, 2$ are produced by the EBG structures in which L_i is the inductance due to the current flowing through the vias and C_i represents the capacitance established between the EBG patch and the metallic radiator ground plane.

The inductance (L) and capacitance (C) are however obtained from the relationship

$$L = \mu_o h \quad (10)$$

$$C = W\epsilon_o \frac{(\epsilon_r + 1)}{\pi} \cosh^{-1} \frac{(2W + g)}{g} \quad (11)$$

where μ_o is permeability of free space, h is the substrate thickness, W is the EBG patch width, ϵ_o is the permittivity of free space, ϵ_r is the relative permittivity of the substrate and g is the gap between the EBG patch and the feed line.

The method of suspended transmission line (MoSTL) is used to analyze the resonant behaviour of the EBG cells, where the EBG cells are positioned under the transmission line in between the two substrates layers. Only one EBG cell is adequate for simulation due to the periodic nature of the cell, hence EBG1 is used in this analysis for clarity purposes but same is true of EBG2. Parametric study is carried out to establish the capacity of the EBG cells to govern the notch frequency.

Figure 2(a), shows that increasing the patch width E_w , increases the capacitance C_i from equation (11) which result in lowering the resonant frequency from equation (9). On the other hand, from Figure 2(b), it is observed that an increase in the vias radius V_r , reduces the inductance and hence an increase in resonant frequency from equation (9). Likewise from Figure 2(c), a decrease in resonant frequency is observed when the gap between the transmission line and the EBG patch g_1 is decreased. This indicates that the closer the EBG patch is to the feed line, the more the coupling between them and hence a better S_{21} magnitude but at the expense of resonant frequency.

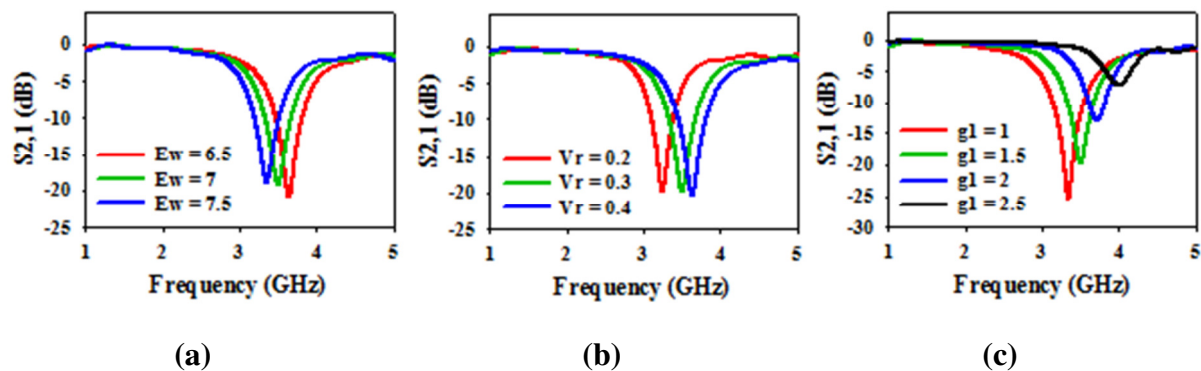


Fig. 2. Effect of variation of (a) Patch Width E_w (b) Via radius V_r and (c) distance between EBG patch and feed line g_1 , against frequency for EBG₁

3. Results and Discussion

The antennas were fabricated and the simulated and measured results are compared. Figure 3 shows a snapshot of the fabricated antennas. Measurement was conducted with a Rohde & Schwarz ZNB40 Vector Network Analyzer (VNA). Figure 4 shows the plot of the reflection coefficient against frequency for the conventional AVA and the band-notch AVA. It is observed that there is good agreement between simulated and measured result. The little deviation was due to soldering inefficiencies and effect of measuring environment. The conventional AVA has an impedance bandwidth from 2.78GHz to more than 12GHz. The electrical length of the inner taper profile was lengthened by the application of the exponential slot corrugation which extended the lower cut off frequency from 2.78 GHz to 2.29 GHz. A frequency notch at 3.21–3.80 and 5.12 – 5.80 GHz was also obtained for IEEE 802.16 WiMAX and IEEE 802.11a WLAN applications with the integration of EBG1 and EBG2 respectively.



Fig. 3. Fabricated Antennas (a) Conventional AVA (b) Corrugated AVA and (c) Proposed AVA

Fig. 4. Measured and Simulated Return Loss of the Proposed Antennas

Fig. 5. Simulated and Measured Gain of the Proposed Antennas

Response of the simulated and calculated measured gain of the antennas is shown in Figure 5. The conventional AVA has a gain of 3 – 7.69 dBi with the peak gain realized at 6.5 GHz. The measured gain was however suppressed by 10.6dBi (5.5 to -5.1 dBi) and 11.43 dBi (7.13 to -4.3 dBi)

at the first and second notch band center frequencies respectively due to the effect of the EBG structures. The proposed antenna has a gain of 2.43 – 8.04 dBi which is significantly higher than the conventional AVA due to the effect of the slot corrugations which eliminated the unwanted surface current at the outer edges of the conventional AVA, thereby improved the radiation gain.

From the surface current distribution in Figure 6, uniform surface current amplitude can be observed at all frequencies along the radiating section of the flared arm of the conventional AVA. This indicates that the antenna radiates energy sufficiently at all frequencies. On the other hand, the proposed antenna does not radiate any surface current when the EGBs are activated at their respective resonant frequencies of 3.5 GHz and 5.5 GHz which created the band notch at those frequencies. It can also be observed that, surface current at 7 GHz for the proposed antenna has strong amplitude indicating the limited effect of the EBG structure at this frequency.

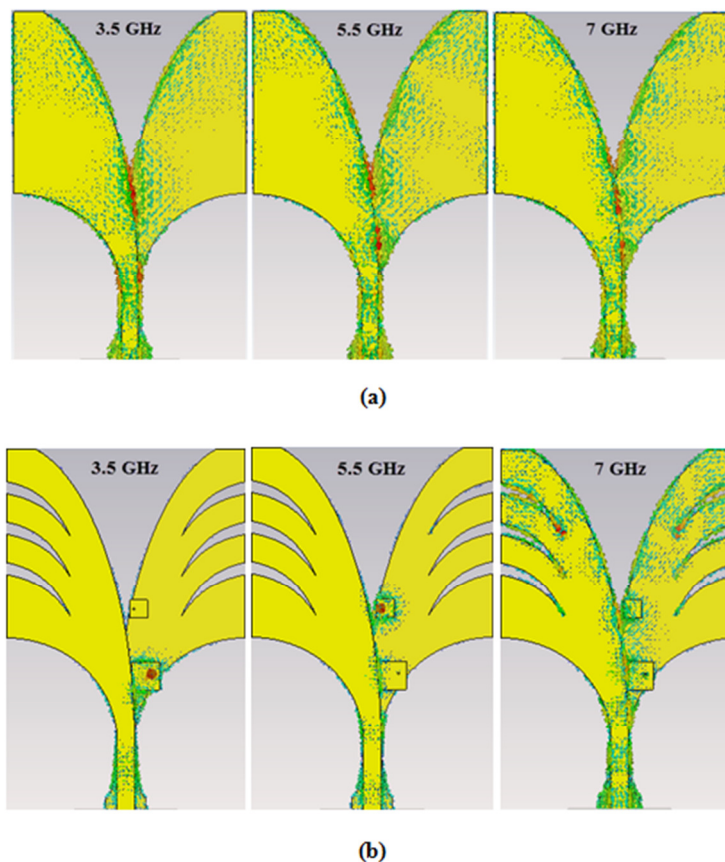


Fig. 6. Surface current distribution at 3.5 GHz, 5.5 GHz & 7 GHz
(a) Conventional AVA and (b) Proposed AVA

The simulated and measured far-field radiation patterns in both E-plane and H-plane at 3.5 GHz, 5.5 GHz and 7 GHz are displayed as shown in Figure 7 with good agreement between the two. Symmetric radiation pattern can be observed in both the principal planes at all frequencies for the conventional antenna while a clear pattern distortion exist with gain attenuation at the notch band frequencies for the proposed antenna due to the incorporation of the EBG structures.

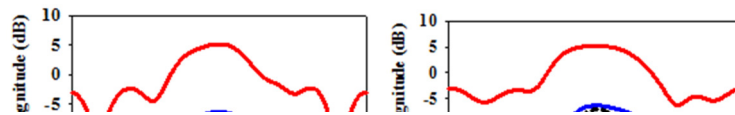


Fig. 7. E-Plane and H-Plane Radiation pattern of conventional and proposed antennas at (a) 3.5 GHz (b) 5.5 GHz & (c) 7 GHz

4. Conclusion

A double-layered band-notch corrugated antipodal Vivaldi antenna was investigated and proposed in this study for ultra-wideband communication systems. With the incorporation of two edge-located vias mushroom EBG structures between the two substrate layers, a dual-band notch at 3.21 – 3.80 GHz and 5.12 – 5.80 GHz for WiMAX and WLAN respectively was achieved. The antenna achieved 2.43 – 8.04 dBi peak realized gain with gain suppression of 10.6 dBi and 11.43 dBi respectively at the two notch bands. Minimal effect of the EBG structure was also observed on the radiation pattern outside the rejected bands. Measured and simulated results of the proposed antennas were in good agreement which proved the suitability of the approach. With simple structure, symmetric and stable end-fire radiation pattern over its operating band, the proposed antenna has proved to be a good choice for band-notch operation in UWB systems.

References

- [1] Federal Communications Commission. "Revision of Part 15 of the Commissions Rules Regarding Ultra-Wideband Transmission Systems. First Report and Order, ET Docket 98-153, FCC 02-48; Adopted: February 14, 2002; Released: April 22, 2002." (2002).
- [2] Li, Yingsong, Wenxing Li, Qiubo Ye, and Raj Mittra. "A survey of planar ultra-wideband antenna designs and their applications." In *Forum for Electromagnetic Research Methods and Application Technologies (FERMAT)*, vol. 1, pp. 1-16. 2014.
- [3] Cicchetti, Renato, Emanuela Miozzi, and Orlandino Testa. "Wideband and UWB antennas for wireless applications: A comprehensive review." *International Journal of Antennas and Propagation* 2017 (2017).
- [4] Dastranj, Aliakbar. "Wideband antipodal Vivaldi antenna with enhanced radiation parameters." *IET Microwaves, Antennas & Propagation* 9, no. 15 (2015): 1755-1760.
- [5] Wang, Ya-Wei, Guang-Ming Wang, and Bin-Feng Zong. "Directivity improvement of Vivaldi antenna using double-slot structure." *IEEE Antennas and Wireless Propagation Letters* 12 (2013): 1380-1383.
- [6] Namas, Tarik, and Moamer Hasanovic. "Ultrawideband antipodal Vivaldi antenna for road surface scanner based on inverse scattering." *Proc. of 28th Annual Review of Progress in Applied Computational Electromagnetics* (2012): 882-887.
- [7] Alhawari, Adam Reda Hasan, Alyani Ismail, Mohd Adzir Mahdi, and Raja Syamsul Azmir Raja Abdullah. "Antipodal Vivaldi antenna performance booster exploiting snug-in negative index metamaterial." *Progress In Electromagnetics Research* 27 (2012): 265-279.
- [8] De Oliveira, Alexandre M., Marcelo B. Perotoni, Sergio T. Kofuji, and João F. Justo. "A palm tree antipodal Vivaldi antenna with exponential slot edge for improved radiation pattern." *IEEE Antennas and Wireless Propagation Letters* 14 (2015): 1334-1337.
- [9] Fei, Peng, Yong-Chang Jiao, Wei Hu, and Fu-Shun Zhang. "A miniaturized antipodal Vivaldi antenna with improved radiation characteristics." *IEEE antennas and wireless propagation letters* 10 (2011): 127-130.
- [10] Zhu, Fuguo, and Steven Gao. "Compact elliptically tapered slot antenna with non-uniform corrugations for ultra-wideband applications." *Radioengineering* 22, no. 1 (2013): 276-280.
- [11] Lazaro, A., R. Villarino, and D. Girbau. "Design of tapered slot Vivaldi antenna for UWB breast cancer detection." *Microwave and Optical Technology Letters* 53, no. 3 (2011): 639-643.
- [12] Deng, Changjiang, Wenhua Chen, Zhijun Zhang, Yue Li, and Zhenghe Feng. "Generation of OAM radio waves using circular vivaldi antenna array." *International Journal of Antennas and Propagation* 2013 (2013).
- [13] Moosazadeh, Mahdi, Sergey Kharkovsky, Joseph Toby Case, and Bijan Samali. "Miniaturized UWB antipodal Vivaldi antenna and its application for detection of void inside concrete specimens." *IEEE Antennas and Wireless Propagation Letters* 16 (2017): 1317-1320.
- [14] de Oliveira, Alexandre M., João F. Justo, Marcelo B. Perotoni, Sérgio T. Kofuji, Alfredo G. Neto, Regis C. Bueno, and Henri Baudrand. "A high directive K och fractal V ivaldi antenna design for medical near-field microwave imaging applications." *Microwave and Optical Technology Letters* 59, no. 2 (2017): 337-346.
- [15] Moosazadeh, Mahdi, Sergey Kharkovsky, Joseph T. Case, and Bijan Samali. "Improved radiation characteristics of small antipodal Vivaldi antenna for microwave and millimeter-wave imaging applications." *IEEE Antennas and Wireless Propagation Letters* 16 (2017): 1961-1964.
- [16] Moosazadeh, Mahdi, Sergey Kharkovsky, Joseph T. Case, and Bijan Samali. "UWB antipodal vivaldi antenna for microwave imaging of construction materials and structures." *Microwave and Optical Technology Letters* 59, no. 6 (2017): 1259-1264.
- [17] Pandey, G. K., H. S. Singh, P. K. Bharti, A. Pandey, and M. K. Meshram. "High gain Vivaldi antenna for radar and microwave imaging applications." *International Journal of Signal Processing Systems* 3, no. 1 (2015): 35-9.
- [18] Elboushi, A., D. Joanes, M. Derbas, S. Khaled, A. Zafar, S. Attabibi, and A. R. Sebak. "Design of UWB antenna array for through-wall detection system." In *Wireless Technology and Applications (ISWTA), 2013 IEEE Symposium on*, pp. 349-354. IEEE, 2013.
- [19] Reddy, K. Aravinda, S. Natarajamani, and S. K. Behera. "Antipodal Vivaldi antenna UWB antenna with 5.5 GHz band-notch characteristics." In *Computing, Electronics and Electrical Technologies (ICCEET), 2012 International Conference on*, pp. 821-824. IEEE, 2012.
- [20] John, Matthias, Max J. Ammann, and Patrick McEvoy. "UWB Vivaldi antenna based on a spline geometry with frequency band-notch." In *Antennas and Propagation Society International Symposium, 2008. AP-S 2008. IEEE*, pp. 1-4. Ieee, 2008.
- [21] Yao, Li, Jun Xiao, Hua Zhu, Nan Li, and Xiuping Li. "A high gain UWB Vivaldi antenna with band notched using capacitively loaded loop (CLL) resonators." In *Microwave and Millimeter Wave Technology (ICMMT), 2016 IEEE International Conference on*, vol. 2, pp. 820-822. IEEE, 2016.

-
- [22] Zhu, Fuguo, Steven Gao, Anthony TS Ho, Raed A. Abd-Alhameed, Chan H. See, Jianzhou Li, and Jiadong Xu. "Miniaturized tapered slot antenna with signal rejection in 5–6-GHz band using a balun." *IEEE antennas and wireless propagation letters* 11 (2012): 507-510.
- [23] Yang, Zhou, Huang Jingjian, and Yuan Naichang. "An antipodal Vivaldi antenna with band-notched characteristics for ultra-wideband applications." *AEU-International Journal of Electronics and Communications* 76 (2017): 152-157.
- [24] Alshamaileh, K. A., M. J. Almalkawi, and V. K. Devabhaktuni. "Dual band-notched microstrip-fed Vivaldi antenna utilizing compact EBG structures." *International Journal of Antennas and Propagation* 2015 (2015).